Anisotropic exciton relaxation in nanostructured metal (Zn and $F_{16}Zn$)-phthalocyanine

Hyeyoung Ahn,[1,*] Wei-Hyun Liou,[1] Huang-Ming Philip Chen,[1] and Chia-Hung Hsu[2]

[1]*Department of Photonics and Institute of Electro-Optical Engineering, National Chiao Tung University, Hsinchu 30010, Taiwan*

[2]*National Synchrotron Radiation Research Center, Hsinchu 300, Taiwan*

[*]*hyahn@mail.nctu.edu.tw*

Abstract: We report ultrafast excited state dynamics of zinc phthalocyanine and zinc hexadecafluoro phthalocyanine thin films which have nanorod-like structures. Excitons in the singlet states undergo multi-exponential relaxation processes to the ground state and the singlet lifetime within a few tens of picoseconds is attributed to the diffusion-limited exciton annihilation process. Diffusive migration of the singlet excitons shows the anisotropic lifetimes depending on the polarization of probe beam. Similar anisotropy is observed in the X-ray diffraction data which exhibits long-range alignment of molecular columns along the long axis of nanorod, whereas disordered arrangement in lateral direction to the axis of nanorod.

OCIS codes: (320.7150) Ultrafast spectroscopy; (160.4236) Nanomaterials.

References and links

1. V. S. Williams, S. Mazumda, N. R. Armstrong, Z. Z. Ho, and N. Peygharmbarian, "Femtosecond dynamics in organic thin films of fluoro-aluminium phthalocyanine," J. Phys. Chem. **96**, 4500 (1992).
2. A. Terasaki, M. Hosoda, T. Wada, H. Tada, A. Koma, A. Yamada, H. Sasabe, A. F. Garito, and T. Kobayashi, "Femtosecond spectroscopy of vanadyi phthalocyanines in various molecular arrangements," J. Phys. Chem. **96**(25), 10534–10542 (1992).
3. V. Gulbinas, M. Chachisvilis, L. Valkunas, and V. Sundstrom, "Excited state dynamics of phthalocyanine films," J. Phys. Chem. **100**(6), 2213–2219 (1996).
4. L. Howe and J. Z. Zhang, "Ultrafast studies of excited-state dynamics of phthalocyanine and zinc phthalocyanine tetrasulfonate in Solution," J. Phys. Chem. A **101**(18), 3207–3213 (1997).
5. J. Zhou, J. Mi, R. Zhu, B. Li, and S. Qian, "Ultrafast excitation relaxation in titanylphthalocyanine thin film," Opt. Mater. **27**(3), 377–382 (2004).
6. V. Gulbinas, "Transient absorption of photoexcited titanylphthalocyanine in various molecular arrangements," Chem. Phys. **261**(3), 469–479 (2000).
7. S. Kakade, R. Ghosh, and D. K. Palit, "Excited state dynamics of Zinc–phthalocyanine nanoaggregates in strong hydrogen bonding solvents," J. Phys. Chem. C **116**(28), 15155–15166 (2012).
8. H.-M. P. Chen, Y.-H. Chen, and B.-R. Lin, "Titanyl phthalocyanine organic thin film transistors with highly π-π interactions," MRS Proceedings, **1270**, 1270–II06–46 (2010).
9. J. S. Louis, D. Lehmann, M. Friedrich, and D. R. T. Zahn, "Study of dependence of molecular orientation and optical properties of zinc phthalocyanine grown under two different pressure conditions," J. Appl. Phys. **101**(1), 013503 (2007).
10. W.-S. Liou, Ultrafast carrier dynamics and hexadecafluorinated zinc phthalocyanine and zinc phthalocyanine, Master Thesis, The National Chiao Tung University, July 2014.
11. S. Senthilarasu, Y. B. Hahn, and S.-H. Lee, "Structural analysis of zinc phthalocyanine (ZnPc) thin films: X-ray diffraction study," J. Appl. Phys. **102**(4), 043512 (2007).
12. L. Li, Q. Tang, H. Li, X. Yang, W. Hu, Y. Song, Z. Shuai, W. Xu, Y. Liu, and D. Zhu, "An ultra-closely p-stacked organic semiconductor for high performance field-effect transistors," Adv. Mater. **19**(18), 2613–2617 (2007).
13. D. Placencia, W. Wang, J. Gantz, J. L. Jenkins, and N. R. Armstrong, "Highly photoactive titanyl phthalocyanine polymorphs as textured donor layers in organic solar cells," J. Phys. Chem. C **115**(38), 18873–18884 (2011).
14. Z. Li, X. Zhang, C. F. Woellner, and G. Lu, "Understanding molecular structure dependence of exciton diffusion in conjugated small molecules," Appl. Phys. Lett. **104**(14), 143303 (2014).
15. H. R. Kerp, H. Donker, R. B. M. Koehorst, T. J. Schaafsma, and E. E. van Faassen, "Exciton transport in organic dye layers for photovoltaic applications," Chem. Phys. Lett. **298**(4-6), 302–308 (1998).

#230634 - $15.00 USD Received 12 Dec 2014; revised 29 Jan 2015; accepted 29 Jan 2015; published 3 Feb 2015

16. P. Peumans, A. Yakimov, and S. R. Forrest, "Small molecular weight organic thin-film photodetectors and solar cells," J. Appl. Phys. **93**(7), 3693 (2003).
17. L. D. A. Siebbeles, A. Huijser, and T. J. Savenije, "Effects of molecular organization on exciton diffusion in thin films of bioinspired light harvesting molecules," J. Mater. Chem. **19**(34), 6067 (2009).
18. R. Signerski and G. Jarosz, "Diffusion length of singlet excitons in copper phthalocyanine films," Photonics Lett. Poland **3**, 107 (2011).
19. M. C. Fravventura, J. Hwang, J. W. A. Suijkerbuijk, P. Erk, L. D. A. Siebbeles, and T. J. Savenije, "Determination of singlet exciton diffusion length in thin evaporated C_{60} films for photovoltaics," J. Phys. Chem. Lett. **3**(17), 2367–2373 (2012).
20. JCPDS-ICDD stands for the joint committee on powder diffraction standards-the international center for diffraction data.

1. Introduction

Due to its superior properties including ultrafast response, thermal and chemical stability, and flexible processing, phthalocyanine (Pc) molecules with the conjugated π-electron system have been widely investigated for use in various optoelectronic devices [1–7]. Pcs are two-dimensional aromatic molecules with an inner ring, and various kinds of metals can be coordinated to the center of rings. Thus, the chemical and electronic properties of metallophthalocyanines (MPcs) can be tuned through the variation of the metal center and the molecular arrangement. MPcs, in particular zinc phthalocyanine (ZnPc) complexes, are of particular interest for photovoltaic and photoconductivity applications due to their high absorption coefficient in a wide spectral range of solar radiation and high energy conversion efficiency.

Attributed to its low-dimensional molecular structure, intermolecular charge transfer in Pcs is possible and it is well known that the energy relaxation of the photoexcited bound electron-hole pair, the exciton, is critically dependent of the molecular arrangement in molecular assemblies [2–7]. The exciton relaxation of monomeric form of Pc molecule in solution is different from that in solid film with ordered stacking of molecular columns. Typically, MPc gives the island growth and does not form a thin continuous film, and the morphology and the domain-size in the solid films are sensitive to the growth conditions. Therefore, the exciton relaxation in the solid films depends on not only the microscopic molecular structures, but also the details of morphology of films. Although there have been several reports on the excition relaxation in thin Pc films, their dependence on the size and the orientation of molecular arrangement within nanostructures remains unknown. In this work, by means of ultrafast time-resolved pump-probe spectroscopy, we investigated the effects of morphology on the excitation energy relaxation in the nanostructured ZnPc and zinc hexadecafluoro phthalocyanine (F_{16}ZnPc) films. Transient transmittance responses measured at different probe wavelengths and polarizations enabled us to understand the various optical absorption and relaxation processes. Strong polarization-dependent relaxation times were observed for ZnPc and F_{16}ZnPc nanorod (NR) films, indicating that exciton relaxation processes are governed by not only the size of NRs, but also the molecular arrangement and orientation within confined nanostructures.

2. Experimental methods

The ZnPc and F_{16}ZnPc films were fabricated on glass substrate for transmittance measurement. All Pc films were deposited using the thermal evaporation method under the vacuum pressure of 3×10^{-6} Torr and the substrate temperature at room temperature. The details of the film preparation method can be found elsewhere [8]. The morphologies and size distribution of each film were analyzed using a field-emission scanning electron microscopy (FE-SEM). Figure 1(a) and 1(b) are top-view and 1(c) and 1(d) are side-view SEM images of ZnPc and F_{16}ZnPc films, respectively, exhibiting nanostructures with different diameters. Despite being grown under a similar growth condition, ZnPc nanorods are close-packed and have a nearly uniform size (diameter~40 nm, length~83 nm), while nanorod-like F_{16}ZnPc nanostructures have tapered shape with a reduced diameter (10–15 nm). To investigate the

#230634 - $15.00 USD Received 12 Dec 2014; revised 29 Jan 2015; accepted 29 Jan 2015; published 3 Feb 2015

anisotropic behavior of exciton recovery in nanostructures, we prepared two F_{16}ZnPc films with different nanorod lengths, ~50 nm and 125 nm, but with similar diameter.

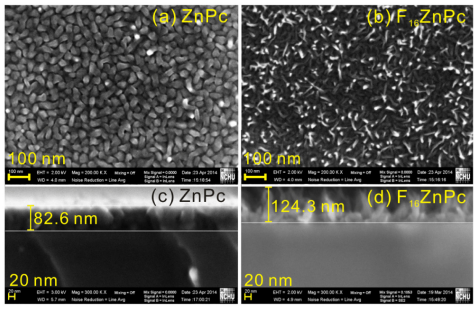

Fig. 1. Top-view [(a) and (b)] and side-view [(c) and (d)] FE-SEM images of ZnPc and F_{16}ZnPc films. ZnPc nanorods are closely packed with the average diameter of ~40 nm, whereas the diameters of F_{16}ZnPc nanorods are getting smaller with a taper-shape.

Ultrafast pump-probe measurements were performed using a Ti:sapphire laser system, which delivers ~150 fs optical pulses at a central wavelength tunable from 740 to 1040 nm. The focused spot of the obliquely incident weak probe beam was maintained smaller than that of the pump beam and an optical chopper was used to improve the signal-to-noise ratio. The fluence of the pump beam was typically 0.03–0.15 GW/cm^2 and all the measurements were performed at room temperature. The absorption spectra of samples are measured by an UV-Vis-IR spectrophotometer in the wavelength range of 300 nm–1600 nm. Our Pc samples have two major absorption bands; B-band in the UV spectra and Q-band in the VIS/NIR region. In order to elucidate the absorption kinetics near the absorption edge, laser pulses at 740 and 800 nm were used to create excitons in Q-band of ZnPc and F_{16}ZnPc films, respectively. The angle of incidence of probe beam was set at 60° in order to distinguish inter- and intra-column interactions. Because the component of the electric field in *p*-polarization is parallel to the plane of incidence, it has more access to the interaction between molecular columns, while the component of the electric field in the *s*-polarization is perpendicular to the plane of incidence so that it has access to the intra-column interaction. Therefore, the polarization of the pump and probe beams in our measurements were defined to be either parallel ($R_{\parallel}$) or perpendicular ($R_{\perp}$) to the long axis of nanorod [9]. The arrangement of molecular columns in Pc films was determined using grazing incidence X-ray diffraction (XRD) at beamline BL01C2 of the National Synchrotron Radiation Research Center, Taiwan. The XRD data were taken using X-rays with a wavelength of 1.03321 Å at an incident angle of 0.1 or 0.2°.

3. Results and discussion

First, we studied the absorption of nanostructured ZnPc and F_{16}ZnPc films. While ZnPc is a *p*-type organic semiconductor, F_{16}ZnPc has *n*-type character by introducing electron withdrawing unit, fluorine, to the periphery of the aromatic ring. The unit cell of F_{16}ZnPc film is larger than that of ZnPc because the van der Waals radius of the terminal fluorine atom of F_{16}ZnPc is larger than that of the terminal hydrogen atom of ZnPc. Absorption spectra of ZnPc and F_{16}ZnPc films in Fig. 2 have essentially similar structures except for the differences in the peak wavelength and the absorbance ratio of the peaks. The absorption peak of the F_{16}ZnPc film is largely red-shifted as compared to that of the ZnPc film, and the absorption curve covers a broad spectral range (550–850 nm) of visible spectrum. This makes F_{16}ZnPc an excellent candidate for light harvesting and conversion in photovoltaic devices.

#230634 - $15.00 USD Received 12 Dec 2014; revised 29 Jan 2015; accepted 29 Jan 2015; published 3 Feb 2015

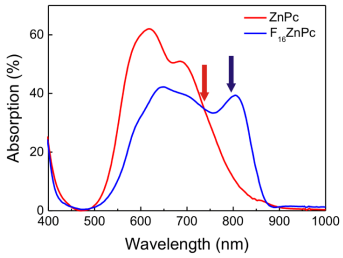

Fig. 2. Absorption spectra of nanostructured ZnPc and F_{16}ZnPc films. Arrows (red for ZnPc and blue for F_{16}ZnPc) indicate the wavelengths of excitation and probe beams used in the time-resolved experiments.

Since ZnPc and F_{16}ZnPc films are consisted of nanostructures, the decay time is expected to be associated with the molecular alignment in small-diameter nanostructures. In order to understand the influence of geometrical shapes on the exciton dynamics in nanostructures, the differential transmittance (DT) of ZnPc and F_{16}ZnPc films are measured with the probe beam whose electric field is either parallel or perpendicular to the long axis of nanorod. Figure 3 illustrates the polarization-dependence of normalized DT for ZnPc and F_{16}ZnPc films photoexcited at 0.06 GW/cm^2. As soon as the pump pulse arrives, DT signals sharply increase and then slowly recover to the ground state. The positive DT reflects the significant bleaching of the optical transitions by the pump-induced exciton population. Relaxation of excitons to the ground state can be described by multiple exponential processes with characteristic lifetimes, τ_1, τ_2, and τ_3.

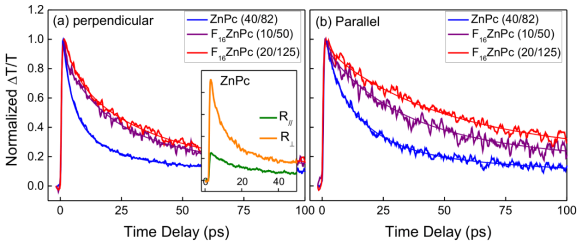

Fig. 3. Normalized DT of the probe electric field (a) perpendicular and (b) parallel to the long axis of nanorod in ZnPc film and F_{16}ZnPc films. The inset shows the *unnormalized* DT for ZnPc.

The exciton lifetimes are calculated from the best fit (solid lines) to DT curves in Fig. 3 and listed in Table 1. The initial ultrafast exciton decay has been observed in many Pcs, and is typically assumed to be an ultrafast bimolecular process, such as electron-phonon scattering or exciton–exciton annihilation with a lifetime of 0.5–5 ps [2–6]. Exciton decay time (τ_2) measured in a few tens of picoseconds can be attributed to several phenomena; the exciton relaxation from the singlet excited states (S_1) to triplet states (T_1) via intersystem crossing (ISC) process, internal conversion (IC) from S_1 to S_0, or vibrational relaxation of excited state electrons in the first excited singlet states (S_1 to S_1). At a low excitation density, exciton-exciton annihilation is not a dominant decay process of S_1 excitons. Instead, it has been found that the diffusion-induced exciton annihilation dominates the decay process from S_1 to S_0 [7]. A long-lifetime component (τ_3) retains more than 400 ps, and the limit of our temporal scanning range prevents us from an accurate determination of τ_3 in our experiment.

Figure 3 shows that the recovery of ultrafast bleaching is polarization dependent, in which the exciton decay processes of $R_{\parallel}$-signals are significantly slower than those of $R_{\perp}$-signals. For the F_{16}ZnPc films with different nanorod heights, $R_{\parallel}$-signals show a clear dependence on geometrical factor given by aspect ratio (width/height), while $R_{\perp}$ signals show nearly the

#230634 - $15.00 USD Received 12 Dec 2014; revised 29 Jan 2015; accepted 29 Jan 2015; published 3 Feb 2015

same exciton relaxation for both samples. For the ZnPc film, the decay time of $R_{\parallel}$-signal is again slower than that of $R_{\perp}$ signal. However, the polarization dependent τ_2 of the ZnPc film is much shorter than those of the F_{16}ZnPc films. This may partly be attributed to the selection of pump/probe wavelength which is either near the absorption peak or near the bottom of the absorption band. Most of Pcs show faster exciton decay when they are excited and probed near the bottom of the absorption band [1,3,5,6]. In our experiment, due to the tunability of our laser system, the exciton kinetics of ZnPc is studied at 740 nm, much below the maximum absorption, while that of F_{16}ZnPc is studied at 800 nm, near the peak of the absorption band [10]. In a separate experiment, we indeed observed much faster decay time for the F_{16}ZnPc films excited at 860 nm.

Table 1. The singlet exciton lifetimes (τ_2) of ZnPc and F_{16}ZnPc films

Sample / Lifetime	F_{16}ZnPc I (20/125)	F_{16}ZnPc II (10/50)	ZnPc (40/83)
$\tau_2\left(R_{\parallel}\right)$ (ps)	48.2	33.2	15.8
$\tau_2\left(R_{\perp}\right)$ (ps)	28.4	27.5	13.7

The anisotropic polarization dependence of exciton decay can be described by the exciton diffusion process. ZnPc and F_{16}ZnPc molecules are planar molecules with short interplanar distances. In solid phase films, disc-like Pc molecules assemble in columns and are inclined relative to the axis of the stack to form herringbone-type structure [6,11–13]. The excitons in Pcs cannot migrate freely in all three directions of space and exciton decay process are diffusion-limited. Diffusion-driven exciton kinetics with the lifetime of a few tens of ps describes the relaxation of population in the singlet excited state S_1. The diffusion of excitons in nanostructures is influenced by the surroundings, such as spatial confinement on the microscopic level by walls of nanostructures, and it is different from that of monomeric Pc. While the lifetime of the S_1 state for monomeric Pc is typically very long, much faster lifetime (27 ps) has been reported for ZnPc nanoaggregates [7]. In typical photovoltaic devices with a planar bilayer configuration, one of the factors to limit their efficiency is the exciton diffusion length (L_e). Exciton diffusion length is related to the exciton lifetime (τ_e) by the diffusion coefficient (D_e) according to the formula: $L_e = \sqrt{D_e \tau_e}$. While D_e depends on exciton hopping rates between different excited states, τ_e depends on exciton decay rates of the excited states [14]. Luminescence and photocurrent measurements are often used to measure L_e of Pcs [15–19]. For ZnPc, the exciton diffusion length has been found to be about 30 nm [13], and for ZnPc nanoaggregates, L_e is known to be ~85 nm and D_e to be 0.43 cm^2/s [13]. Without independent knowledge of the diffusion coefficient, we cannot estimate a precise value for the exciton diffusion length of our nanostructured Pc samples. However, the nanorod height-dependent exciton lifetime along $R_{\parallel}$-direction for the F_{16}ZnPc films indicates that L_e of the F_{16}ZnPc films can be longer than the height of the shorter nanorod film (50 nm). Meanwhile, diffusive exciton motion can also be limited via the trapping by impurities and the imperfections of the molecular arrangement. Therefore, better understanding on the crystalline structure is required.

According to the XRD patterns of the F_{16}ZnPc and ZnPc films in Fig. 4, the nanostructured films have sharp diffraction peaks at 2θ = 4.221° and 4.615°, which correspond to the interplanar space between columnar stacking axes d = 14.03 and 12.83Å, respectively. The measured value of d for nanostructured ZnPc is similar to 12.90 Å for typical herringbone stacking of ZnPc [20]. Larger d for the F_{16}ZnPc film is attributed to larger molecular size. The narrow diffraction curves suggest that both films have the long-range crystallinity and molecular columns are almost regularly stacked along the nanorod axis (normal to the substrate). In contrast, XRD signal in the in-plane direction (parallel to the substrate) is nearly isotropic except a small peak at 5.021° (d = 11.80 Å) for ZnPc. This result

#230634 - $15.00 USD Received 12 Dec 2014; revised 29 Jan 2015; accepted 29 Jan 2015; published 3 Feb 2015

suggests that Pc columns are consisted of micro-size domains and their orientations are random along $R_{\perp}$-direction. Meanwhile, those singlet excitons that perform a random walk in nanorods may encounter traps, such as structural defects, which rapidly deactivate excitons. Structural defects can be largely concentrated in the space between the micro-domains and limit the exciton diffusion.

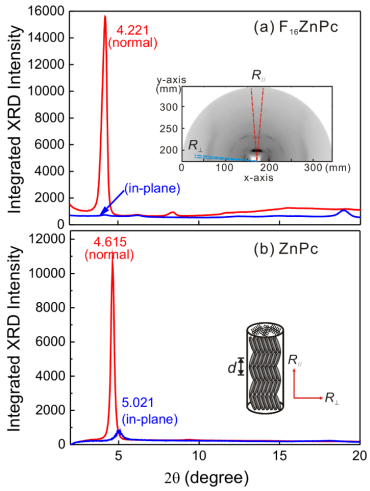

Fig. 4. X-ray diffraction curves for (a) F_{16}ZnPc and (b) ZnPc films measured in the direction normal- and parallel to the substrate plane. The inset in Fig. 4(a) shows the azimuthal angle dependence of diffraction pattern and the one in Fig. 4(b) pictures the schematic of molecular arrangement within a nanorod. The bending at the tip as well as the tapered shape of F_{16}ZnPc nanorods may be responsible for the large background and the appearance of extra peaks in the XRD curves.

By the way, the inset in Fig. 3 shows that the unnormalized DT of $R_{\perp}$-signal is much larger than that of $R_{\parallel}$-signal. This result reveals that despite the random molecular orientation of micro-domains, more excitons are generated within the π-stacks of Pcs in $R_{\perp}$ direction, but their recovery processes are limited by the morphological parameters.

4. Summary

In summary, we demonstrated the ultrafast exciton dynamics in vertically aligned ZnPc and F_{16}ZnPc nanostructures. The ground state bleaching near the Q-band edge followed by multi-exponential recovery was commonly observed for ZnPc and F_{16}ZnPc nanorods. The diffusive migration of singlet excitons before annihilation dominates the exciton dynamics. The singlet exciton lifetime shows a strong dependence on the length of nanorods as well as the polarization of the probe beam. Longer exciton lifetime along the axis of nanorod implies the diffusive migration of excitons through the molecular columns stacked parallel to the substrate. In lateral direction to the axis of nanorod, the diffusion of excitons is limited by randomly oriented molecular columns. These results suggest the evidence of anisotropic growth of Pc molecules in nanostructures and identify the anisotropic singlet exciton lifetimes in Pc organic materials. Finally, this work provides a full understanding of dynamics of excitons in nanostructured organic materials and the reduced singlet exciton diffusion within nanostructures offer their potentials in small-molecule photovoltaic devices.

Acknowledgment

This work was supported by the National Science Council (NSC 101-2112-M-009-012-MY3) and the Science Vanguard Research Program (NSC-103-2628-M-007-001) in Taiwan.

#230634 - $15.00 USD Received 12 Dec 2014; revised 29 Jan 2015; accepted 29 Jan 2015; published 3 Feb 2015